ADVANCED MATERIALS
www.advmat.de

www.MaterialsViews.com

Porous Carbon Spheres from Energetic Carbon Precursors using Ultrasonic Spray Pyrolysis

*Hangxun Xu, Jinrui Guo, and Kenneth S. Suslick**

Porous carbon materials have unique physicochemical properties and are used extensively in gas storage and separation, water treatment, catalysis, fuel cell electrodes, capacitors, and batteries.[1–13] Most porous carbons are prepared by carbonization of raw natural materials (e.g., wood, coal, and nutshells, etc.)[1,2,14–16] New methods of making porous carbons via carbonization of block copolymers, sugars, or resorcinol-formaldehyde resin aerogels have also been developed.[17–21] Structurally rigid inorganic templates like silica, metal-organic frameworks and zeolites have been used to prepare porous carbons, although such sacrificial templates prove to be cumbersome and expensive.[22–25] The control over structure and morphology of porous carbon is significantly limited compared to polymeric materials, nanostructured metals or metal oxides, and silica-based materials whose structures and morphologies can be conveniently tailored by the colloidal synthesis.[26–31] Aerosol synthesis methods have been extensively utilized to prepare a variety of metal and metalloid oxides,[32–44] generally in spherical morphologies, but occasionally with unusual nanostructures;[45–50] aerosol syntheses have been widely used in industry for fine powder production and thin film deposition because the process is simple and can be easily scaled up for mass production. We have previously developed a continuous, one-step and template-free aerosol approach using ultrasonic spray pyrolysis (USP) to prepare porous carbon spheres using either halogenated carboxylate salts (e.g., alkali chloroacetates) or simple carbohydrates (e.g., sucrose);[49–51] a schematic of the USP apparatus is setup is shown in the Supporting Information (Figure S1 in the Supporting Information). In this work, we expand the aerosol synthesis of porous carbon materials with unusual morphologies by the use of energetic carbon precursors, specifically alkali propiolates ($HC{\equiv}CCO_2M$, M = Li, Na, and K). The resulting hierarchically porous carbons show some unprecedented carbon structures including Janus, jellyfish, and bowl-like microstructures.

Metal propiolates are a class of energetic materials (the C≡C bond contains ≈490 kJ/mol more energy than the C–C bond) and contain facile leaving groups (e.g., CO, CO_2, or C_2H_2) via decarbonylation or decarboxylation process.[52] In general, the decomposition process can be described as:

$$HC{\equiv}CCO_2M \rightarrow M_2CO_3 + CO + CO_2 + C_2H_2 + C \quad (M = Li, Na, and K)$$

Dr. H. X. Xu, J. R. Guo, Prof. K. S. Suslick
Department of Chemistry
University of Illinois at Urbana-Champaign
Urbana, IL 61801, USA
E-mail: ksuslick@illinois.edu

DOI: 10.1002/adma.201201915

They can polymerize to poly(propiolate) salts when exposed to heat, X- or γ-ray irradiation.[53,54] Once mixed with strong oxidants they become potentially explosive (Warning: propiolate salts are energetic materials and must be kept away from heat and strong oxidants.). Another intriguing feature of metal propiolates is that the different cations induce changes in the propiolate thermal decomposition, i.e., they decompose at different temperatures, they produce different amounts of gases during decomposition, and the undergo different thermolysis reactions (e.g., decarbonylation vs decarboxylation).[52]

Figure 1 shows the scanning electron microscope (SEM) and transmission electron microscope (TEM) images of porous carbon spheres produced using 1 M solutions of $HC{\equiv}CCO_2Li$, $HC{\equiv}CCO_2Na$, and $HC{\equiv}CCO_2K$ respectively at a decomposition temperature of 700 °C. Figure S2 shows lower magnification SEM images of above prepared carbons. The structure of porous carbon spheres produced in this way varies with the choice of the corresponding alkali salts. Aerosolized liquid droplets containing $HC{\equiv}CCO_2Li$ produce porous carbon spheres in a thin carbon shell (Figure 1A,B). The decomposition of $HC{\equiv}CCO_2Na$ leads to the formation of hollow carbon spheres with large pores inside the carbon shell (Figure 1B,E). Carbon spheres decomposed from $HC{\equiv}CCO_2K$ exhibit similar structures similar to those from $HC{\equiv}CCO_2Li$ but with larger inner pores (Figure 1C,F). Porous carbon spheres prepared from different alkali salts show similar type-IV isotherms with high microporosity (Figure S3). The Brunauer–Emmett–Teller (BET) surface areas, pore volumes via Barrett–Joyner–Halenda (BJH) method, morphologies and high temperature mass loss during formation of porous carbon spheres from different alkali salts and their mixtures are given in **Table 1**. The highest surface area attained in porous carbon spheres from K salts is due to the formation of microporous structures as revealed by rapid increase of adsorbed volume at relatively low pressure and the pore size distribution via the BJH method (Figure S4).

The porous carbon materials that result from the thermolysis of the alkali propiolates can take on several different morphologies that are dependent on the choice of propiolate cations (Figures 1, **2**, **3**, and S5–8). This phenomenon is caused by the differences in the thermal decomposition of the precursors, which were probed by simultaneous TGA and DSC (**Figures 4** and S9). Let us consider the correlation of the TGA/DSC with the resulting morphologies first for each of the pure cations (Figure 1) and then for the mixed cations (Figures 2,3, and S5–8). The factors that are important in these processes include (1) the melting point of the precursor, (2) the initial temperature of decomposition, and (3) the relative amount of gases produced at *higher* temperatures as the carbon network becomes fully formed. The melting point of the precursors vs. the decomposition temperature determines whether a core of molten salt will

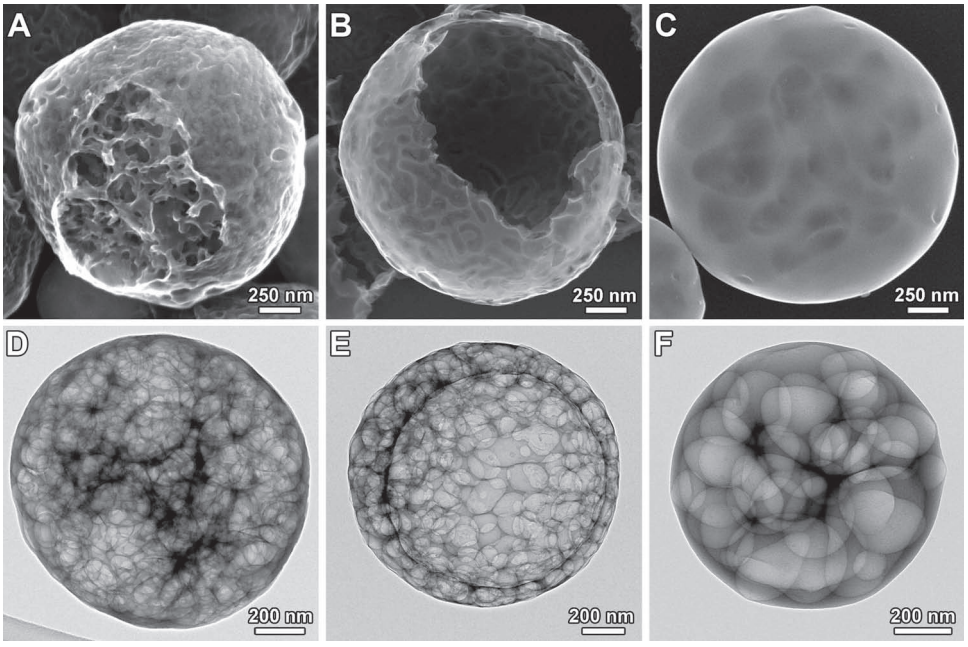

Figure 1. SEM and TEM images of porous carbon spheres prepared by USP of 1 M solutions of (A and D) $HC{\equiv}CCO_2Li$, (B and E) $HC{\equiv}CCO_2Na$, and (C and F) $HC{\equiv}CCO_2K$.

be formed, which leads to a hollow microsphere. The relative amount of gas released at higher temperatures than the initial decomposition determines the microporosity (and hence the main contribution to the total surface area) as the carbon shell becomes fully condensed, crosslinks, and hardens.

For $HC{\equiv}CCO_2Li$ (Figures 1A,D and S2A), melting of the precursor occurs just before its rapid decomposition at 222 °C, as indicated by the negative dip in the DSC. The dramatic mass loss (≈70%) during the decomposition of $HC{\equiv}CCO_2Li$ indicates that this is a very rapid process that results in relatively low microporosity of the resulting carbon. Only large pores are created as the carbon forms around the initially produced Li_2CO_3 which serves as a temporary template. Very small amounts of gaseous products (e.g., CO_2, CO, and C_2H_2) are

Table 1. Summary of porous carbons prepared from different compositions of alkali propiolates.

Composition of precursor	Product morphology	Surface area [m^2/g]	Initial decomposition temperature [°C]	Mass loss after initial decomposition [%]	Micropore volume [cm^3/g]	Mesopore volume [cm^3/g]
$HC{\equiv}CCO_2Li$ [1 M]	macroporous microspheres	118	222	7	0.01	0.05
$HC{\equiv}CCO_2Na$ [1 M]	hollow microporous microspheres	723	210	22	0.05	0.15
$HC{\equiv}CCO_2K$ [1 M]	microporous microspheres	865	192	13	0.03	0.05
$HC{\equiv}CCO_2Li$ [0.25 M] $HC{\equiv}CCO_2Na$ [0.75 M]	Janus microporous microspheres	488	202	13	0.02	0.07
$HC{\equiv}CCO_2Li$ [0.25 M] $HC{\equiv}CCO_2K$ [0.75 M]	nested bowl double-hemispheres	551	172	16	0.04	0.05
$HC{\equiv}CCO_2Li$ [0.33 M] $HC{\equiv}CCO_2Na$ [0.33 M] $HC{\equiv}CCO_2K$ [0.33 M]	hollow microporous microspheres	434	174	23	0.03	0.04

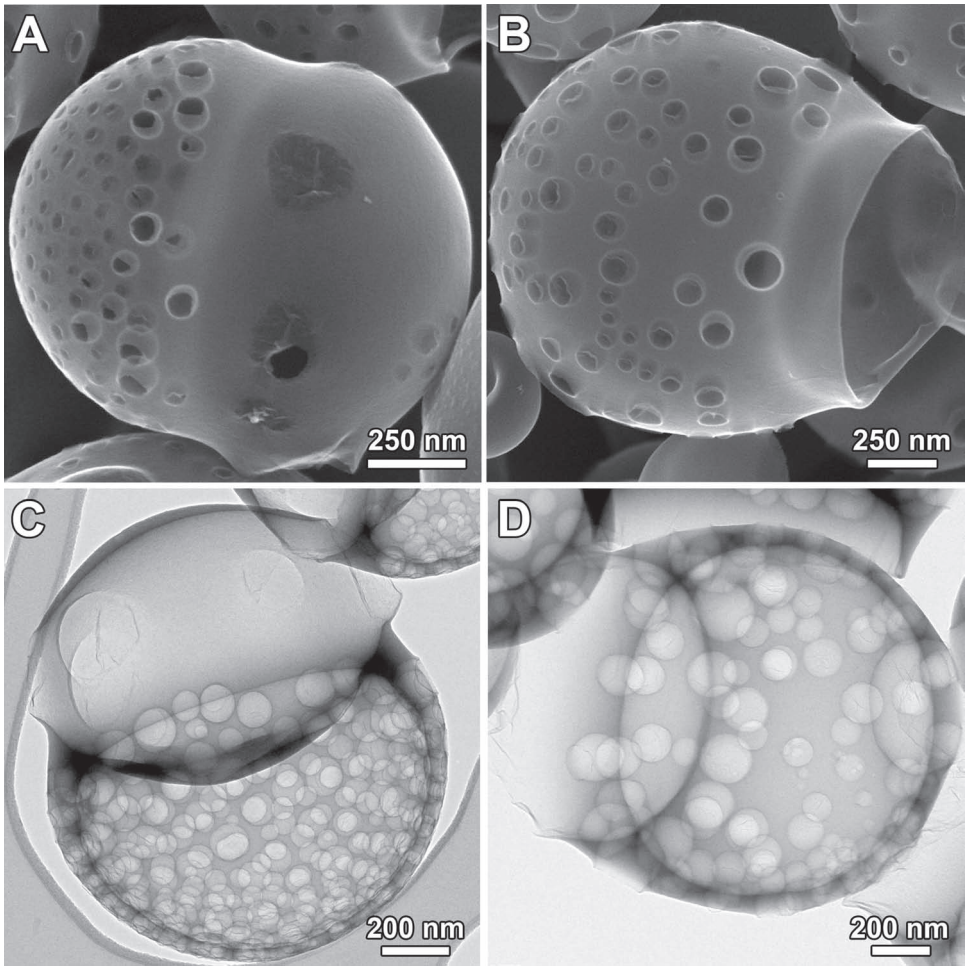

Figure 2. SEM images at lower and higher magnification of porous carbon spheres prepared from (A and C) 0.25 M HC≡CCO_2Li and 0.75 M HC≡CCO_2Na, which give Janus spheres, and (B and D) 0.75 M HC≡CO_2Li and 0.25 M HC≡CCO_2Na, with a jelly-fish morphology from the blow-out of the presumed Janus shape initially formed.

released at higher temperatures, insufficient to generate significant microporosity in the nearly fully-formed carbon structure.

For HC≡CCO_2Na (Figures 1B,E and S2B), melting of the precursor again occurs just before decomposition starts at 210 °C. The decomposition continues until 500 °C, so the molten salts can serve as a template core. In contrast to the Li salt, however, the microporous carbon slowly forms over this molten core and produces a high surface area shell; significant amounts of gaseous byproducts are released at higher temperature as the carbon solid undergoes decarboxylation, condensation, and crosslinking processes at higher temperatures which provides for microporosity in the final product.

For HC≡CCO_2K (Figures 1C,F and S2C), no melting occurs before the decomposition at 192 °C, so as a result, the porous

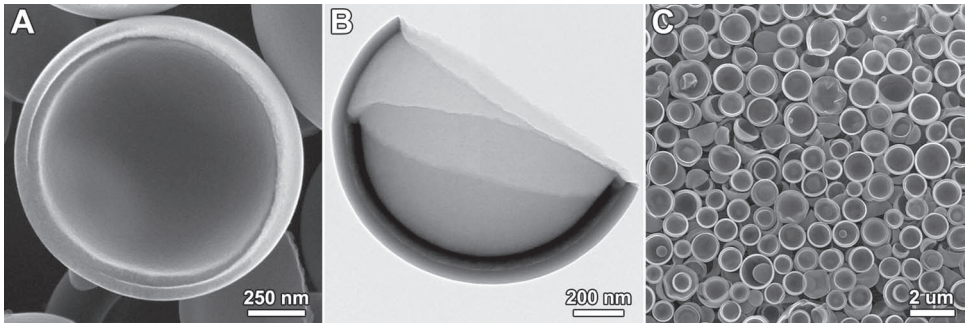

Figure 3. (A) SEM and (B) TEM images of porous carbon double-hemispheres prepared from 0.25 M HC≡CCO_2Li and 0.75 M HCC≡CO_2K. (C) Low magnification SEM image of a monolayer of the carbon double-hemispheres formed by slow evaporation of an ethanol solution on a silicon wafer.

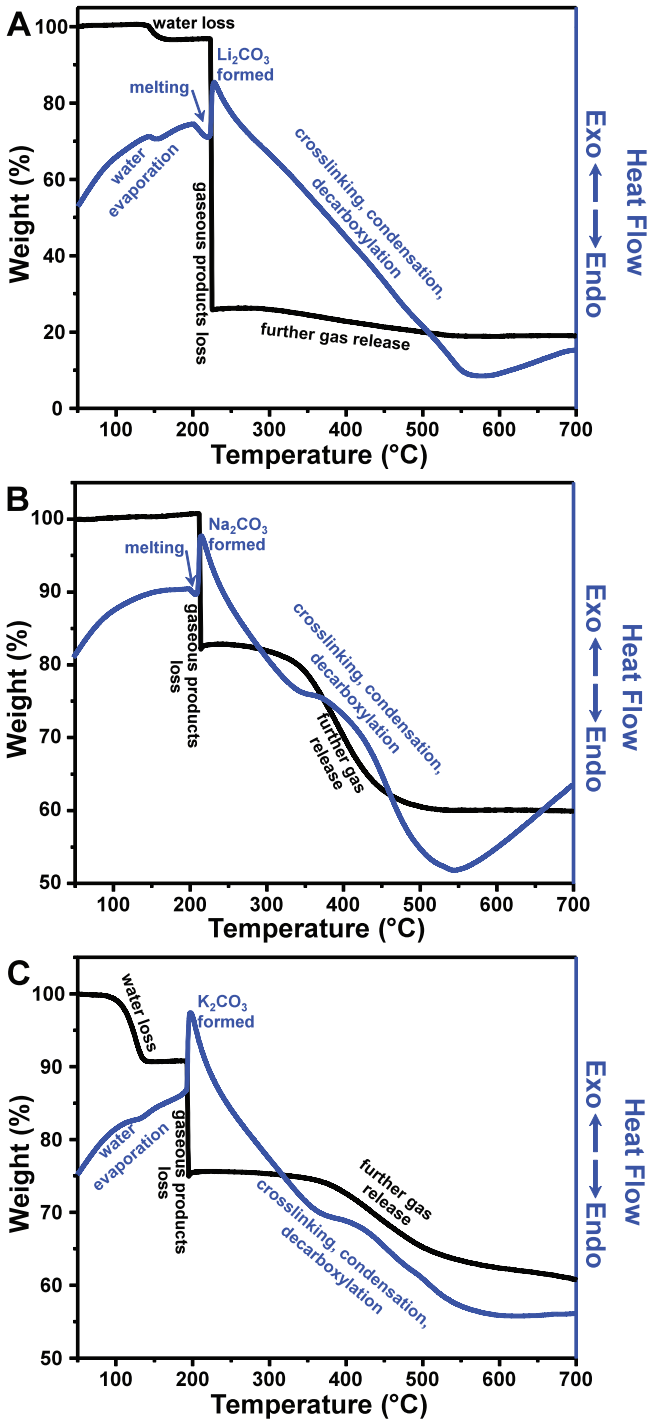

Figure 4. Simultaneous TGA (black, left axis) and DSC (blue, right access) plots for decomposition under Ar atmosphere (10 °C/min) of (A) HC≡CCO_2Li, (B) HC≡CCO_2Na, and (C) HC≡CCO_2K.

carbon network is produced through solid-state reactions. The diffusion of precursor in the carbon network is limited and large pores are produced during the initial rapid thermal decomposition. Microporosity and consequent high surface areas are formed due to the release of more gaseous products at higher temperatures as full crosslinking occurs.

Surprisingly, dramatically different structures and morphologies emerge if *mixed* alkali salts are used as precursors. Figure 2 shows representative SEM and TEM images of porous carbon spheres produced from mixed HC≡CCO_2Li/HC≡CCO_2Na solutions. When a 0.25 M HC≡CCO_2Li and 0.75 M HC≡CCO_2Na solution is used as the precursor, Janus carbon spheres with different surface texture and pore sizes on each hemisphere are obtained (Figures 3A,C). Jellyfish-like carbon spheres are produced if the concentration of HC≡CCO_2Li is increased from 0.25 to 0.75 M (Figure 3B,D). SEM images of carbon spheres before washing show that the pores are filled with inorganic salts formed during the decomposition of organic ligand (Figure S5).

When a solution of 0.25 M HC≡CCO_2Li and 0.75 M HC≡CCO_2K is used as the precursor, nested-bowl carbon double-hemispheres are obtained (Figure 4). Interestingly, in essentially all cases, there is a smaller bowl trapped in the slightly larger outer bowl. Carbon spheres collected at the end of furnace tube before washing, however, exhibit intact spherical morphology with a salt core (Figure S6), which means that the nested-bowl structure is formed from the spherical carbon spheres. This observation, together with cracks on the edge of carbon bowls, indicates that the double-bowl carbon structure is formed from the inward collapse of one half of the initially-formed thin-shelled carbon spheres upon dissolution of the salt core during work-up. More than 90% of microspheres are formed with a nested-bowl hemispherical structure while the remaining microspheres still maintain an intact closed spherical shell or are slightly collapsed. Interestingly, by the slow evaporation of a diluted ethanol solution on a silicon wafer, we can self-assemble these carbon bowls into a uniformly oriented monolayer with all bowls opening up (Figure 3C and S7).

When HC≡CCO_2Li, HC≡CCO_2Na, and HC≡CCO_2K are mixed at a ratio of 1:1:1, hollow microporous carbon spheres can be obtained (Figure S8). The N_2-sorption measurement of these hollow carbon spheres exhibits a type-IV isotherm and a surface area of 433 m^2/g (Table 1). BJH pore size distribution indicates that the majority of the pores are between ≈3–10 nm. Hollow carbon spheres have been demonstrated to be excellent catalyst supports and promising electrode materials for lithium-ion batteries.[55–57] Compared to the typical templating approach that is used to prepare hollow carbon spheres,[58–60] our aerosol synthesis method does not require the tedious templates synthesis (e.g., using colloidal silica) and subsequent removal steps. Instead, the inorganic salts formed in situ during precursor decomposition act as temporary templates and can be easily washed out during workup.

The mechanism for the formation of such dramatically different morphologies from pyrolysis of mixed energetic alkali propiolates is difficult to explain due to the complex thermal decomposition behaviors of these precursor mixtures. Some insights, however, can be derived from the TGA/DSC of these mixtures (Figure S9). For example, mixed 1:3 HC≡CCO_2Li/HC≡CCO_2Na shows a single sharp decomposition peak at 202 °C (Figure S9A), which is lower than that of the individual alkali propiolates. Surprisingly, no melting event is observed before decomposition when the two salts are mixed, although melting occurs before the thermal decomposition of Li or Na

propiolate alone. The formation of Janus particles (Figure 2A,C) suggests the likelihood of a phase separation before the decomposition between a Li^+/Na^+ eutectic and excess $HC{\equiv}CCO_2Na$. When the composition contains more Li^+ than Na^+, the smooth side of the Janus particle blows out, resulting in the jellyfish-like morphology observed (Figure 2B,D). The macroporous side of the Janus or jellyfish particles (i.e., left side in Figure 2A,B) therefore arises from the Li^+/Na^+ eutectic decomposition, the smooth side (i.e., right side in Figure 2A) derives from the Na salt and the blown out side (i.e., right side of Figure 2B) from the Li salt.

In addition to propiolate salts, the acetylenedicarboxylates (i.e., $O_2CC{\equiv}CCO_2$ dianions) can also be used as carbon precursors for preparation of porous carbon spheres. The SEM and TEM images of porous carbon spheres produced from pyrolysis of the alkali salts of acetylenedicarboxylic acid are shown in Figure S10.

Porous carbon microspheres produced in this approach are amorphous by powder XRD both before and after annealing at 800 °C (Figure S11). Solid state MAS ^{13}C NMR of carbon spheres produced from $HC{\equiv}CCO_2K$ shows one resonance peak at ≈130 ppm corresponding to polyaromatic carbon atoms (Figure S12).[61] Two small resonance peaks around 60 ppm and 195 ppm can be assigned to acetylenic groups and carboxylic or ketonic groups respectively.[61] This observation is consistent with the results from infrared spectroscopy (Figure S13). The absorption at 3450 cm^{-1} corresponds to the υ(O–H) stretch from hydroxyl groups. The weak absorption at 3150 cm^{-1} is from aromatic C–H. There is an absorption at 1630 cm^{-1} from υ(C=C) and an absorption at 1380 cm^{-1} from anti-symmetric carboxylic acid vibrational modes.[60,61] The surface functional groups were also evaluated by X-ray photoelectron spectroscopy (XPS) (Figure S14), which confirms the existence of carbonyl and carboxylate groups on the surfaces of the porous carbon microspheres. Bulk elemental analysis (Table S1) reveals that the carbon spheres contain ≈75–90 wt% C, ≈1–2 wt% H, and ≈10–25 wt% O (by difference). Raman spectra of such porous carbon spheres contain two broad peaks at ≈1360 cm^{-1} and ≈1600 cm^{-1} which are consistent with defect (D) and graphitic bands (G) (Figure S15). The D bond is the disordered peak characteristic of sp^3 bonded amorphous carbon while the G bond is characteristic of well-ordered, crystalline sp^2 bonded carbon. The ratio of D and G bands can be taken as a measurement of the relative crystallinity of a carbon material.[64,65] Raman analysis of the D:G ratio for porous carbon spheres synthesized by USP of alkali propiolates shows that the there is no dramatic difference between different carbon spheres prepared from different alkali precursors.

The morphologies that we observe derive from the microdroplet reactors that the USP technique produces and not simply from the high reactivity of the alkali propiolate precursors. In contrast, decomposition of bulk precursor results in the formation of very fragile carbon foams (Figures S16 and S17) and not to the formation of any porous spheres. The aerosol droplets generated by the ultrasonic nebulization act as isolated microreactors inside the hot furnace and confine the decomposition gases within the evolving microspheres with the subtleties of the specific thermal decomposition pathways of different precursors determining the morphology of the final products. If one assumes the contribution of one carbon atom per propiolate (i.e., complete loss of CO_2 and alkali metal ion), the theoretical yields found for the production of carbon microspheres are 29, 24 and 39% for Li, Na, and K salts (i.e., $HC{\equiv}CO_2M$), respectively.

In summary, a convenient synthetic approach to prepare porous carbon spheres with unique and unprecedented morphologies has been demonstrated using energetic carbon precursors via ultrasonic spray pyrolysis. The unique decomposition behaviors of alkali propiolates and their mixtures lead to dramatically different carbon structures and morphologies. Engineering the porous carbon spheres can be achieved through controlling the compositions of precursors without using templates. The high surface area and unique porous structures suggest that they may prove useful as electrode materials, adsorbents, catalyst supports, or for other applications by integrating other functional materials into their pores.[66–68]

Experimental Section

Preparation of Porous Carbon Spheres: The USP setup used in this work is shown in Figure S1. The operating frequency of the water nebulizer is 1.65 MHz. The furnace was preheated to the desired temperature (700 °C, unless otherwise noted). Argon was used as the carrier gas at a flow rate of 1 L/min, which was used to purge the system of air for 30 min prior to the addition of the precursor solution. The black powders after the pyrolysis were collected in water bubblers, washed and centrifuged with deionized water at least 5 times to remove alkali salts formed during synthesis. The final products were dried overnight in a vacuum oven at 60 °C. Propiolic acid ($HC{\equiv}CO_2H$, 95%), lithium hydroxide monohydrate (99.995%), sodium hydroxide (99.99%), and potassium hydroxide (99.99%) were purchased from Sigma-Aldrich and used as received. The precursor solutions were prepared by first dissolving the appropriate amount of propiolic acid in water and then adding a stoichiometric amount of an alkali hydroxide solution (e.g., LiOH, NaOH, and KOH). Suspensions were sonicated for 5 min and then stirred for 1 h to achieve homogeneous solutions. All solutions were prepared at room temperature. Warning: Propiolate salts are energetic materials and must be kept away from heat and strong oxidants.

Characterization of Porous Carbon Spheres: TEM images were taken with a JEOL 2100 transmission electron microscope with an accelerating voltage of 200 kV. SEM images were taken using a Hitachi S4800 field-emission scanning electron microscope with an accelerating voltage of 10 kV. Samples for SEM images were prepared by placing a droplet of ethanol solutions of porous carbon spheres on a Si wafer and drying at room temperature. Thermal gravimetric analysis (TGA) and differential scanning calorimetry (DSC) was conducted on a TA Instruments Q600-SDT Simultaneous DSC-TGA, with a heating rate of 10 °C/min under Ar. FT-IR spectra were recorded on a Thermo-Nicolet Nexus 670 spectrometer. X-ray powder diffractograms were collected using Cu Kα radiation (λ = 1.5418 Å) with a Siemens-Bruker D5000 instrument operating at 40 kV and 30 mA. X-ray photoelectron spectra were collected using a X-ray photoelectron microscope (XPS, Physical Electronics, Mg Kα source). Raman spectra were obtained directly from a thin film of graphene or carbon samples deposited onto a Si wafer excited with a 532 nm laser. Solid state ^{13}C NMR spectra were recorded on a Varian Unity Inova 300 spectrometer. N_2 isotherms and surface area measurements were performed on a Quantachrome Instruments Nova 2200e Surface Area and Pore Analyzer; carbon samples were degassed under vacuum at 130 °C for 12 h before analysis. Bulk elemental analyses were performed by the UIUC School of Chemical Sciences Microanalysis Laboratory using an Exeter Analytical, Inc. Model CE-440 CHN analyzer and a Perkin-Elmer-Sciex Elan DRCe ICP-MS for the alkali metal analyses.

Supporting Information

Supporting Information is available from the Wiley Online Library or from the author.

Acknowledgements

This work is supported by the U.S. NSF DMR 09-06904. This research was carried out in part in the Center for Microanalysis of Materials, UIUC, which is partially supported by the U.S. Department of Energy under grant DE-FG02-07ER46453 and DE-FG02-07ER46471.

Received: May 11, 2012
Revised: May 18, 2012
Published online: August 24, 2012

[1] R. C. Bansal, J. B. Donnet, F. Stoeckli, *Active Carbon*, Marcel Dekker, New York **1988**.
[2] *Porosity in Carbons: Characterization and Applications* (Ed: J. W. Patrick), Halsted Press, New York **1995**.
[3] S. Sircar, In *Adsorption by Carbons* (Eds: E. J. Bottani, J. M. D. Tascon), Elsevier, Oxford **2008,** pp. 565–592.
[4] Y. F. Zhai, Y. Q. Dou, D. Y. Zhao, P. F. Fulvio, R. T. Mayes, S. Dai, *Adv. Mater.* **2011**, *23*, 4828.
[5] E. Frackowiak, F. Beguin, *Carbon* **2001**, *39*, 937.
[6] C. Moreno-Castilla, J. Rivera-Utrilla, *MRS Bull.* **2001**, *26*, 890.
[7] G. Newcombe, in *Adsorption by Carbons* (Eds: E. J. Bottani, J. M. D. Tascon), Elsevier, Oxford **2008,** pp. 679–709.
[8] A. L. Dicks, *J. Power Source* **2006**, *156*, 128.
[9] B. C. Steele, A. Heinzel, *Nature* **2001**, *414*, 345.
[10] Z. Yang, Y. Xia, R. Mokaya, *J. Am. Chem. Soc.* **2007**, *129*, 1673.
[11] J. Fan, T. Wang, C. Z. Yu, B. Tu, Z. Y. Jiang, D. Y. Zhao, *Adv. Mater.* **2004**, *16*, 1432.
[12] A. S. Arico, P. Bruce, B. Scrosati, J. M. Tarascon, W. V. Schalkwijk, *Nat. Mater.* **2005**, *4*, 366.
[13] Y. Yu, L. Gu, C. Zhu, P. A. Aken, J. Maier, *J. Am. Chem. Soc.* **2009**, *131*, 15984.
[14] F. Rodriguez-Reinoso, M. Molina-Sabio, *Carbon* **1992**, *30*, 1111.
[15] Z. Hu, E. F. Vansant, *Carbon* **1995**, *33*, 561
[16] M. S. Tam, M. J. Antal, *Ind. Eng. Chem. Res.* **1999**, *38*, 4268.
[17] J. Lee, J. Kim, T. Hyeon, *Adv. Mater.* **2006**, *18*, 2073.
[18] C. Liang, Z. Li, S. Dai, *Angew. Chem. Int. Ed.* **2008**, *47*, 3696.
[19] A. Stein, Z. Wang, M. A. Fierke, *Adv. Mater.* **2009**, *21*, 265.
[20] A. M. Elkhatat, S. A. Al-Muhtaseb, *Adv. Mater.* **2011**, *23*, 2887.
[21] S. Schrettl, R. Szilluwit, H. Frauenrath, *Angew. Chem. Int. Ed.* **2010**, *49*, 6496
[22] S. Kubo, R. Demir-Cakan, L. Zhao, R. J. White, M. M. Titirici, *ChemSusChem* **2010**, *3*, 188.
[23] Y. Xia, Z. Yang, Z. R. Mokaya, *Nanoscale* **2010**, *2*, 639.
[24] J. Lee, S. Han, T. Hyeon, *J. Mater. Chem.* **2004**, *14*, 478.
[25] B. Sakintuna, Y. Yürüm, *Ind. Eng. Chem. Res.* **2005**, *44*, 2893.
[26] Y. N. Xia, Y. J. Xiong, B. Lim, S. E. Skrabalak, *Angew. Chem. Int. Ed.* **2009**, *48*, 60.
[27] Y. N. Xia, P. D. Yang, Y. G. Sun, Y. Y. Wu, B. Mayers, B. Gates, Y. D. Yin, F. Kim, H. Q. Yan, *Adv. Mater.* **2003**, *15*, 353.
[28] U. Jeong, X. W. Teng, Y. Wang, H. Yang, Y. N. Xia, *Adv. Mater.* **2007**, *19*, 33.
[29] C. J. Brinker, Y. F. Lu, A. Sellinger, H. Y. Fan, *Adv. Mater.* **1999**, *11*, 579.
[30] Y. W. Jun, J. S. Choi, J. Cheon, *Angew. Chem. Int. Ed.* **2006**, *45*, 3414.
[31] Y. D. Yin, A. P. Alivisatos, *Nature* **2005**, *437*, 644.
[32] T. T. Kodas, M. J. Hampden-Smith, *Aerosol Processing of Materials*, John Wiley & Sons, New York **1999**.
[33] Y. F. Lu, H. Y. Fan, A. Stump, T. L. Ward, T. Rieker, C. J. Brinker, *Nature* **1999**, *398*, 223.
[34] J. H. Bang, K. S. Suslick, *Adv. Mater.* **2010**, *22*, 1039.
[35] C. Boissiere, D. Grosso, A. Chaumonnot, L. Nicole, C. Sanchez, *Adv. Mater.* **2010**, *23*, 599.
[36] W. H. Suh, K. S. Suslick, *J. Am. Chem. Soc.* **2005**, *127*, 12007.
[37] D. Majumdar, T. T. Kodas, H. D. Glicksman, *Adv. Mater.* **1996**, *8*, 1020.
[38] J. H. Kim, T. A. Germer, G. W. Mulholland, S. H. Ehrman, *Adv. Mater.* **2002**, *14*, 518.
[39] L. Li, C. K. Tsung, Z. Yang, G. D. Stucky, L. D. Sun, J. F. Wang, C. H. Yan, *Adv. Mater.* **2008**, *20*, 903.
[40] J. H. Bang, R. J. Helmich, K. S. Suslick, *Adv. Mater.* **2008**, *20*, 2599.
[41] S. S. Dunkle, R. J. Helmich, K. S. Suslick, *J. Phys. Chem. C* **2009**, *113*, 11980.
[42] K. Okuyama, W. Lenggoro, *Chem. Eng. Sci.* **2003**, *58*, 537.
[43] S. Y. Lee, L. Gradon, S. Janeczko, F. Iskandar, K. Okuyama, *ACS Nano* **2010**, *84*, 541.
[44] L. Li, C. K. Tsung, T. Ming, Z. H. Sun, W. H. Ni, Q. Shi, G. D. Stucky, J. F. Wang, *Adv. Funct. Mater.* **2008**, *18*, 2956.
[45] W. H. Suh, A. R. Jang, Y. H. Suh, K. S. Suslick, *Adv. Mater.* **2006**, *18*, 1832.
[46] A. B. D. Nandiyanto, K. Okuyama, *Adv. Powder Technol.* **2011**, *22*, 1.
[47] A. K. Mann, S. E. Skrabalak, *Chem. Mater.* **2011**, *26*, 8804.
[48] C. K. Tsung, J. Fan, N. F. Zheng, Q. H. Shi, A. J. Forman, J. F. Wang, G. D. Stucky, *Angew. Chem. Int. Ed.* **2008**, *47*, 8682.
[49] S. E. Skrabalak, K. S. Suslick, *J. Am. Chem. Soc.* **2006**, *128*, 12642.
[50] S. E. Skrabalak, K. S. Suslick, *J. Phys. Chem. C* **2007**, *111*, 17807.
[51] M. E. Fortunato, M. Rostam-Abadi, K. S. Suslick, *Chem. Mater.* **2010**, *22*, 1610.
[52] C. E. Stoner, T. B. Brill, *Inorg. Chem.* **1989**, *28*, 4500.
[53] T. Masuda, M. Kawai, *Polymer* **1982**, *23*, 744.
[54] B. E. Davidov, B. A. Krentsel, G. V. Kchutareva, *J. Polym. Sci. Part C: Polym. Symp.* **1967**, *16*, 1365.
[55] F. P. Hu, Z. Y. Wang, Y. L. Li, C. M. Li, X. Zhang, P. K. C, *J. Power Sources* **2008**, *177*, 61.
[56] K. T. Lee, Y. S. Jung, S. M. Oh, *J. Am. Chem. Soc.* **2003**, *125*, 5652.
[57] W. M. Zhang, J. S. Hu, Y. G. Guo, S. F. Zhang, L. S. Zhong, W. G. Song, L. J. Wan, *Adv. Mater.* **2008**, *20*, 1160.
[58] A. M. Herring, J. T. McKinnon, B. D. McCloskey, J. Filley, K. W. Gneshin, R. A. Pavelka, H.-J. Kleebe, D. J. Aldrich, *J. Am. Chem. Soc.* **2003**, *125*, 9916.
[59] F. B. Su, X. S. Zhao, Y. Wang, L. K. Wang, J. Y. Lee, *J. Mater. Chem.* **2006**, *16*, 4413.
[60] R. J. White, K. Tauer, M. Antonietti, M. M. Titirici, *J. Am. Chem. Soc.* **2010**, *132*, 17360.
[61] J. C. C. Freitas, F. G. Emmerich, G. R. C. Cernicchiaro, L. C. Sampaio, T. J. Bonagamba, *Solid State Nucl. Magn. Reson.* **2001**, *20*, 61.
[62] E. Fuente, J. A. Menendez, M. A. Diez, D. Suarez, M. A. Montes-Moran, *J. Phys. Chem. B* **2003**, *107*, 6350.
[63] *Chemistry and Physics of Carbon* (Ed: L. R. Radovic), Marcel Dekker, New York **2001**.
[64] Y. Wang, D. C. Alsmeyer, R. L. McCreery, *Chem. Mater.* **1990**, *2*, 557.
[65] J. Schwan, S. Ulrich, V. Batori, H. Ehrhardt, S. R. P. Silva, *J. Appl. Phys.* **1996**, *80*, 440.
[66] J. H. Bang, K. Han, S. E. Skrabalak, H. Kim, K. S. Suslick, *J. Phys. Chem. C* **2007**, *111*, 10959.
[67] J. D. Atkinson, M. E. Fortunato, S. A. Dastgheib, M. Rostam-Abadi, M. J. Rood, K. S. Suslick, *Carbon* **2011**, *22*, 1610.
[68] H. Kim, M. E. Fortunato, H. X. Xu, J. H. Bang, K. S. Suslick, *J. Phys. Chem. C* **2011**, *115*, 20481.